THE JOURNAL OF BIOLOGICAL CHEMISTRY
Vol. 278, No. 44, Issue of October 31, pp. 43628–43635, 2003
Printed in U.S.A.

Parkin-deficient Mice Exhibit Nigrostriatal Deficits but Not Loss of Dopaminergic Neurons*

Received for publication, August 13, 2003
Published, JBC Papers in Press, August 20, 2003, DOI 10.1074/jbc.M308947200

Matthew S. Goldberg‡, Sheila M. Fleming§, James J. Palacino‡, Carlos Cepeda¶, Hoa A. Lam‖, Anushree Bhatnagar, Edward G. Meloni‡, Nanping Wu¶, Larry C. Ackerson‖, Gloria J. Klapstein¶, Mahadevan Gajendiran¶, Bryan L. Roth**, Marie-Françoise Chesselet§, Nigel T. Maidment‖, Michael S. Levine¶, and Jie Shen‡ ‡‡**

*From the ‡Center for Neurologic Diseases, Harvard Medical School, Brigham and Women's Hospital, Boston, Massachusetts 02115, the ¶Mental Retardation Research Center and the Departments of §Neurology and ‖Psychiatry and Biobehavioral Sciences, University of California, Los Angeles, California 90024, and the **Departments of Biochemistry, Psychiatry, and Neurosciences, Case Western Reserve University Medical School, Cleveland, Ohio 44106*

Loss-of-function mutations in parkin are the major cause of early-onset familial Parkinson's disease. To investigate the pathogenic mechanism by which loss of parkin function causes Parkinson's disease, we generated a mouse model bearing a germline disruption in parkin. *Parkin*−/− mice are viable and exhibit grossly normal brain morphology. Quantitative *in vivo* microdialysis revealed an increase in extracellular dopamine concentration in the striatum of *parkin*−/− mice. Intracellular recordings of medium-sized striatal spiny neurons showed that greater currents are required to induce synaptic responses, suggesting a reduction in synaptic excitability in the absence of parkin. Furthermore, *parkin*−/− mice exhibit deficits in behavioral paradigms sensitive to dysfunction of the nigrostriatal pathway. The number of dopaminergic neurons in the *substantia nigra* of *parkin*−/− mice, however, is normal up to the age of 24 months, in contrast to the substantial loss of nigral neurons characteristic of Parkinson's disease. Steady-state levels of CDCrel-1, synphilin-1, and α-synuclein, which were identified previously as substrates of the E3 ubiquitin ligase activity of parkin, are unaltered in *parkin*−/− brains. Together these findings provide the first evidence for a novel role of parkin in dopamine regulation and nigrostriatal function, and a non-essential role of parkin in the survival of nigral neurons in mice.

Parkinson's disease (PD)[1] is an age-related movement disorder characterized by bradykinesia, rigidity, resting tremor, and postural instability. The neuropathologic hallmarks of PD are the loss of dopaminergic neurons in the *substantia nigra* (SN) and the presence of intraneuronal cytoplasmic inclusions known as Lewy bodies. The clinical manifestations of PD are due to progressive degeneration of dopaminergic neurons in the pars compacta of the SN that give rise to the nigrostriatal pathway, causing dopamine (DA) depletion in the striatum, where it is required for normal motor function. Little is known about the mechanisms of PD pathogenesis and nigral degeneration, although DA neurons have been shown to be susceptible to oxidative stress (1), mitochondrial defects (2), and environmental toxins (3).

The recent identification of genes linked to familial forms of PD (FPD) makes it possible to investigate the pathogenic mechanism by employing genetic approaches (4–6). Over fifty recessively inherited mutations, including deletion, frameshift, nonsense, and missense mutations, have been identified in *parkin* in large numbers of families, making *parkin* the major gene responsible for early-onset FPD (7–10). Although the first report linked *parkin* mutations to autosomal recessive juvenile parkinsonism (AR-JP) with atypical clinical features (5), many more cases identified subsequently were considered typical early-onset FPD with symptoms often indistinguishable from sporadic PD (9, 11). Autopsies of limited numbers of patients showed selective loss of dopaminergic neurons in the SN either in the absence (12–15) or in the presence (16) of Lewy bodies. The recessive inheritance mode and variety of *parkin* mutations indicate a loss-of-function pathogenic mechanism.

Parkin is widely expressed in most tissues including brain and heart (5). Although its transcripts are equally abundant in various brain sub-regions, parkin protein is enriched in the SN (5, 17–20). *In vitro* studies have shown that parkin can function as an E3 ubiquitin ligase, mediating the covalent transfer of ubiquitin to protein substrates subject to proteasomal degradation (21–23). However, it is unclear how loss of parkin function leads to nigral degeneration and PD.

To investigate the pathogenic mechanism of PD in an animal model and to elucidate the normal physiological role of parkin *in vivo*, we created a mouse model bearing a targeted germline disruption of parkin. Molecular, histological, neurochemical, electrophysiological, behavioral, and biochemical analyses of *parkin*−/− mice reveal a novel role for parkin in dopamine regulation and nigrostriatal function *in vivo*, and a non-essential role of parkin in the survival of nigral neurons in mice.

EXPERIMENTAL PROCEDURES

Generation of parkin−/− *Mice*—A targeting vector was constructed using 1.8- and 3.5-kb DNA fragments as the 5′ and 3′ homologous sequences, respectively (Fig. 1*A*). A negative selection cassette, PGK-dt, which encodes the diphtheria toxin and has been shown to enhance

* This work was supported by NINDS, National Institutes of Health and the Michael J. Fox Foundation for Parkinson's Research. The costs of publication of this article were defrayed in part by the payment of page charges. This article must therefore be hereby marked "*advertisement*" in accordance with 18 U.S.C. Section 1734 solely to indicate this fact.

‡‡ To whom correspondence should be addressed: Center for Neurologic Diseases, Harvard Institutes of Medicine, 77 Avenue Louis Pasteur, Boston, MA 02115. Tel.: 617-525-5561; Fax: 617-525-5252; E-mail: jshen@rics.bwh.harvard.edu.

[1] The abbreviations used are: PD, Parkinson's disease; DA, dopamine; SN, *substantia nigra*; FPD, familial Parkinson's disease; AR-JP, autosomal recessive juvenile parkinsonism; ACSF, artificial cerebrospinal fluid; RMP, resting membrane potential; AP, action potential; AHP, afterhyperpolarization; PSP, postsynaptic potential; DOPAC, dihydroxyphenylacetic acid; HVA, homovanillic acid; HPLC, high pressure liquid chromatography.

screening efficiency as much as 75-fold (24), was also included. The linearized targeting vector was transfected into J1 (129/Sv) ES cells. After selection in G418, 200 clones were screened by Southern analysis for homologous recombination. Six clones were identified by the presence of the expected 3.7-kb band corresponding to the targeted allele. Using the 3′ external probe and a probe specific for the *neo* sequence, two clones were confirmed to carry the desired homologous recombination events without random insertion. ES cells of both clones were injected into C57BL/6 and Balb/c blastocysts. Chimeric offspring were crossed with C57BL/6 mice to obtain germline transmission, which was confirmed by Southern analysis with the 5′ probe shown in Fig. 1*A*. Heterozygous mice were then interbred to obtain homozygous knockout and wild-type control mice. Mice were subsequently genotyped by PCR using primers (5′-CCTACACAGAACTGTGACCTGG; 5′-GCAGAATTACAGCAGTTACCTGG; 5′-ATGTTGCCGTCCTCCTTGAAGTCG) specific for the wild-type or the targeted allele. The resulting 250 and 500 bp PCR products correspond to the wild-type and targeted alleles, respectively. All experimental procedures were carried out in accordance with the USPHS Guide for Care and Use of Laboratory Animals.

Northern, RT-PCR, and Western—Northern and RT-PCR were performed as previously described (25). For Western blotting, brains were Dounce-homogenized in buffer (0.33 M sucrose, 8 mM HEPES, pH 7.4, Roche complete protease inhibitors for parkin, or 150 mM NaCl, 50 mM Tris, pH 7.4, 0.2% Nonidet P-40, Roche complete protease inhibitors for α-synuclein, synphilin-1 and CDCrel-1) and centrifuged, and the protein content of the supernatant was analyzed by BCA assay (Pierce). Immunoprecipitation of α-synuclein for detection of the glycosylated species was performed essentially as previously described (26) with the following modifications: 10 mg of supernatant was used for the immunoprecipitation of α-synuclein and the IP antibody (KC7071) was used at a 1:10 dilution. For Western blotting, 50 μg of protein was mixed with 2× Laemmli buffer, boiled, and resolved on 10% acrylamide gels (parkin, synphilin-1, and CDCrel-1) or 4–20% gradient gels (α-synuclein) (Invitrogen), transferred to nitrocellulose membranes, blocked in 5% milk in TBST (50 mM Tris, pH 7.4, 150 mM NaCl, 0.1% Tween-20), and incubated with a primary antibody (Parkin, Cell Signaling 2132; 1:1000; CDCrel-1, gift of Dr. William Honer, 1:1000; α-synuclein, Syn-1, BD PharMingen, 1:2000; synphilin-1, gift of Dr. Simone Englender, 1:100) and then a peroxidase-conjugated anti-rabbit (parkin, CDCrel-1, and synphilin-1) or mouse (α-synuclein) antibody (Promega). The membranes were then treated with chemiluminescence reagent (PerkinElmer Life Sciences) and exposed to film. Samples were reprobed with tubulin and actin to confirm equal protein loading.

Histology and Neuron Count—Mouse brains were dissected, formalin fixed for 2 h, processed for paraffin embedding, and sectioned in the coronal plane at 16-μm thickness. Each paraffin block contained 4 *parkin*−/− and 4 wild-type brains. Deparaffinized sections were stained with cresyl violet or tyrosine hydroxylase (TH) antibodies. The number of DA neurons in the SN was determined by counting TH-immunoreactive neurons in coronal sections of four brains per genotype per age group using the fractionator and optical dissector methods of unbiased stereology (27) under a Leica DMRB microscope equipped with a CCD camera connected to a computer running Bioquant image analysis software. The same software was used to measure nigral DA neuron volumes from 4 wild-type and 4 *parkin*−/− brains at the age of 24 months. The experimenter was blind to the genotypes of the mice. Values are reported as means ± S.E. Statistical differences were assessed by Student's *t* test.

Striatal DA Measurements—For striatal tissue DA measurement, striata were dissected and stored at −80 °C. Frozen striata were sonicated in ice-cold 0.1 N perchloric acid, 0.2 mM sodium bisulfite and centrifuged 20 min at 20,000 × *g* at 4 °C to remove debris. The supernatant was filtered (0.2 μm) and applied to a C18 reverse phase HPLC column linked to an ESA model 5200A electrochemical detector.

For no-net-flux microdialysis, *parkin*−/− and wild-type mice were implanted unilaterally under halothane anesthesia with a microdialysis probe (CMA 11, 2-mm membrane length, CMA/Microdialysis, Chelmsford, MA) in the striatum using the following stereotaxic coordinates measured from bregma and the skull surface in mm: rostral +0.6, lateral +1.8, ventral +4.5. Probes were perfused with an artificial cerebrospinal fluid (ACSF: 0.2 mM ascorbic acid, 125 mM NaCl, 2.5 mM KCl, 0.9 mM NaH_2PO_4, 5 mM Na_2HPO_4, 1.2 mM $CaCl_2$, 1 mM $MgCl_2$, pH 7.4) at a flow rate of 0.5 μl/min. After 24 h, DA was incorporated in the microdialysis perfusion medium at 5 different concentrations (0, 5, 10, 20, 40 nM) each for 2 h in random order and dialysate was collected in 30 min. intervals into 1.5 μl of 12.5 mM perchloric acid/250 μM EDTA. Samples were frozen at −70 °C for analysis by HPLC with electrochemical detection (Antec Leyden, Zoeterwoude, The Netherlands) as described previously (28). The difference in DA concentration between the perfusion medium flowing into the probe and that flowing out of the probe ($[DA]_{in} - [DA]_{out}$) was plotted on the *y*-axis against $[DA]_{in}$ on the *x*-axis. A line of best fit was constructed by least-squares analysis. The intercept at the *x*-axis (DA concentration at the point of no net flux) and the slope of the line (the extraction fraction, a measure of DA reuptake) was determined for each animal and differences between genotypes were assessed by Students' *t* test.

Dopamine Receptor Binding Assays—D1 and D2 binding assays were performed with [^{3}H]spiperone and [^{3}H]SCH23390, essentially as previously detailed (29) using crude synaptic membrane fractions prepared from mouse striata (prepared as described in Ref. 30) with ketanserin (100 nM) included to inhibit binding to 5-HT2A/2C serotonin receptors. Protein determinations were performed using the BioRad kit with bovine serum albumin as a standard. Binding data were analyzed with Prism (GraphPad) as previously described (31). Data represent mean ± S.E. of 3–6 separate determinations from striata isolated from wild-type and *parkin*−/− animals. Statistical differences were assessed by Student's *t* test.

Electrophysiology—Detailed electrophysiological procedures were previously described (32). Briefly, mice were anesthetized with halothane, decapitated, brains were placed in ice-cold oxygenated ACSF (in mM: NaCl 130, $NaHCO_3$ 26, KCl 3, $MgCl_2$ 5, NaH_2PO_4 1.25, $CaCl_2$ 1, glucose 10 (pH 7.2–7.4)) and coronal corticostriatal sections (~350 μm) were made so that striatal neurons could be studied both intracellularly and by activation of their main excitatory input from the cortex. Slices were transferred to a submersion recording chamber in which they were perfused constantly with oxygenated ACSF (31–32 °C) in an atmosphere of warm, moist 95% O_2, 5% CO_2. Intracellular responses were recorded using sharp microelectrodes (60–110 MOhms) filled with 3 M potassium acetate, 5 mM KCl, and 2% w/v biocytin to facilitate subsequent examination of the morphology of recorded neurons. Basic passive and active membrane properties (resting membrane potential (RMP), current-voltage relationships, input resistance, action potential (AP) parameters (amplitude and half-amplitude duration), after hyperpolarization (AHP) amplitude) were examined using intracellularly injected current pulses to determine neuronal excitability. Values are reported as means ± S.E. Synaptic responses were evoked with a bipolar stimulating electrode placed in the corpus callosum to activate primarily corticostriatal afferents, the main excitatory pathway into the striatum, which release glutamate. Stimuli of increasing intensity (100-μs duration) were delivered every 5 s and 5 traces at each intensity were averaged. Peak amplitudes of postsynaptic potentials (PSPs) were measured, and input-output relationships were plotted. From each cell, the averaged PSP whose peak amplitude was 50% of maximum on the input-output curve was further analyzed for between-group comparisons of peak amplitudes and half-amplitude durations. Paired-pulse facilitation was assessed by presenting two stimuli, which evoked responses at 50% maximum amplitude 50 ms apart and measuring the ratio of the peak amplitude of the second PSP divided by the first PSP. Biocytin labeling confirmed that all recovered neurons were medium-sized spiny neurons with similar appearance between genotypes.

Behavioral Tests—All tests were performed by investigators blind to the genotypes. For the open field test, individual mice were placed in 42 × 42 cm acrylic animal cages for 15 min during which their horizontal and vertical movements were monitored by 3 arrays of 16 infrared light beam sensors (AccuScan Instruments) and analyzed using AccuScan VersaMax software.

For the rotarod test, mice were placed 4 at a time on an Economex accelerating rotarod (Columbus Instruments) equipped with individual timers for each mouse. Mice were initially trained to stay on the rod at a constant rotation speed of 5 rpm. After a 2-min rest, mice that would fall were repeatedly placed back on the rotarod until they were able to stay on the rotating rod for at least 2 min. Following training, mice were subsequently tested by placing them on the rod at a rotation speed of 5 rpm, as the rod accelerated by 0.2 rpm/sec, the latency to fall was measured. Mice were tested for a total of 3 trials.

For the beam traversal task, a Plexiglas beam (Plastics Zone Inc., Woodland Hills, CA) consisting of four sections (25 cm each, 1 m total length) of varying width (3.5, 2.5, 1.5, and 0.5 cm) was used. To increase the difficulty of the test, a wire mesh cover (1 cm^2) of corresponding width was placed on the beam surface. Mice were trained for 2 days to traverse the beam without the wire mesh to their home cages. On the day of the test, mice were trained further with two trials without the grid overlay and two trials with the wire grid placed on the beam. Mice were then tested for 3 trials by traversing the grid-surfaced beam, and their performance was videotaped. The numbers of steps and slips (a limb slipped through the wire grid during a forward movement) were

counted by viewing the videotapes in slow motion. Fisher's LSD was used for planned comparisons between genotypes.

For the adhesive removal test, small adhesive stimuli of five increasing sizes were placed on the forehead, out of view for the mice. The stimuli consisted of 0.25 and 0.5 inch Avery labels cut in half or whole or combined. To remove the stimulus, mice raised both forelimbs toward their head and swiped off the stimulus with both forepaws within a 60-s trial, after which the experimenter removed the adhesive. Each mouse was given a score equal to the largest size adhesive it was unable to sense and remove, averaged over two trials. Scores were compared between genotypes using a Mann-Whitney *U* test. All mice were able to sense and remove the largest size adhesive, but none could sense and remove the smallest adhesive.

RESULTS

Generation of Parkin-deficient Mice—parkin is a large gene (~2 Mb), which contains 12 exons and encodes a protein of 465 amino acid residues (5, 33). The exon 3 deletion mutation is one of the most common mutations in AR-JP and results in absence of parkin protein (8, 18, 20). Exon 3 contains a non-integral number of codons, thus, deletion of exon 3 results in a frameshift after amino acid 57 and premature termination at a stop codon in exon 4 following 39 additional out-of-frame amino acid residues in humans (8, 18, 20). We therefore chose to target exon 3 to generate a *parkin*-null mutant mouse. A targeting vector was constructed in which most of exon 3 was replaced in-frame by the coding sequence of EGFP, followed by translation and transcription termination sequences and the *PGK-neo* cassette (Fig. 1*A*). The protein sequences predicted to result from wild-type and mutant transcripts are depicted in Fig. 1*B*. Two clones of ES cells carrying the proper homologous recombination events without random integration of the targeting vector were injected into blastocysts. Germline transmission of the targeted allele was confirmed by Southern analysis (Fig. 1*C*). Interbreeding of heterozygous mice gave rise to wild-type, heterozygous, and homozygous knockout (*parkin*−/−) mice at the expected Mendelian ratio.

To determine whether our targeted mutation causes skipping of exon 3, we performed Northern and RT-PCR analyses. Northern analysis of total RNA using a probe specific for exons 4–12 showed a smaller *parkin* transcript in *parkin*−/− brains (Fig. 1*D*). RT-PCR analysis using primers specific for exons 2 and 5 followed by sequencing confirmed that in *parkin*−/− brains exon 2 was spliced to exon 4, skipping exon 3 entirely (Fig. 1*E*). Exon 3 skipping causes a reading frameshift after amino acid 57 and premature termination at a stop codon in exon 5 following 49 additional out-of-frame amino acid residues in mice (Fig. 1*B*). The sensitivity of RT-PCR confirmed the complete absence of intact *parkin* transcripts in *parkin*−/− mice. Sequencing also revealed an aberrant splice product, which results from the use of a cryptic splice acceptor site 3 bases into exon 4, leading to addition of 48 rather than 49 out-of-frame amino acid residues (Fig. 1*B*). Although these truncated *parkin* transcripts are present in *parkin*−/− mice, it is unlikely that functional parkin fragments can be produced from these truncated transcripts. Western analysis using an antiserum raised against the C-terminal region of parkin confirmed the absence of parkin in *parkin*−/− mice (Fig. 1*F*), and ruled out the presence of possible parkin fragments initiated from in-frame ATGs downstream of exon 3, consistent with the notion that reinitiation of translation following a sizable open reading frame is highly unlikely (34).

Since we introduced the *EGFP* cDNA fused in-frame into *parkin* exon 3, which was intended for a reporter system for the *parkin* promoter activity, we also performed Northern analysis using an *EGFP*-specific probe and confirmed the presence of *EGFP* transcripts in *parkin*−/− mice (data not shown). RT-PCR followed by sequencing confirmed that the EGFP coding sequence is intact and fused in-frame to *parkin* exon 3. However, the parkin-EGFP fusion protein was barely detectable by Western analysis (data not shown), perhaps due to the presence of the ubiquitin-like domain of parkin (35).

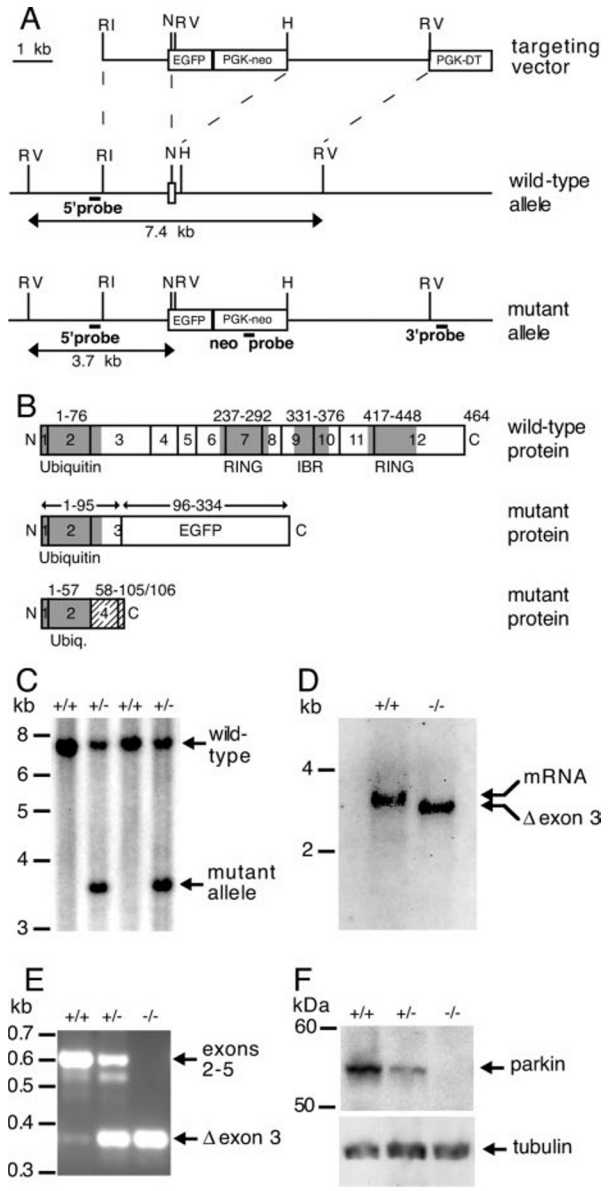

FIG. 1. **Generation and characterization of *parkin*−/− mice.** *A*, schematic representation of the wild-type *parkin* genomic region encompassing exon 3, indicated by a *small open box*, and the targeted allele. The locations of the three probes used for Southern analysis are indicated, along with the sizes of *Eco*RV restriction fragments. Abbreviations: *H*, *Hin*dIII; *N*, *Nde*I; *RI*, *Eco*RI; *RV*, *Eco*RV. *B*, schematic representation of the structure of the expected protein products derived from the wild-type and the targeted alleles. Amino acid residue numbers are shown above relevant domains (*shaded gray*) or frame-shifted sequences (*hatched*). Numbers in *boxes* depict the exons coding for each region. *C*, Southern analysis of tail DNA digested with *Eco*RV and hybridized with the 5′ probe. *D*, Northern analysis of total RNA hybridized with a probe specific for exons 4–12 shows a smaller mRNA species in *parkin*−/− mice. *E*, RT-PCR analysis of *parkin* transcripts using primers specific for exons 2 and 5. *F*, Western analysis of total brain homogenates confirms the reduction and absence of parkin in heterozygous and homozygous mutant mice, respectively. The same blot was incubated with a β-tubulin antibody to normalize loading.

parkin−/− mice are viable and fertile without obvious abnormalities. Open field tests of *parkin*−/− mice revealed no significant alterations in their general behavior and exploratory anxiety (Fig. 2). Nissl staining revealed normal brain morphology in *parkin*−/− mice (Fig. 3, *A* and *B*). Immunohis-

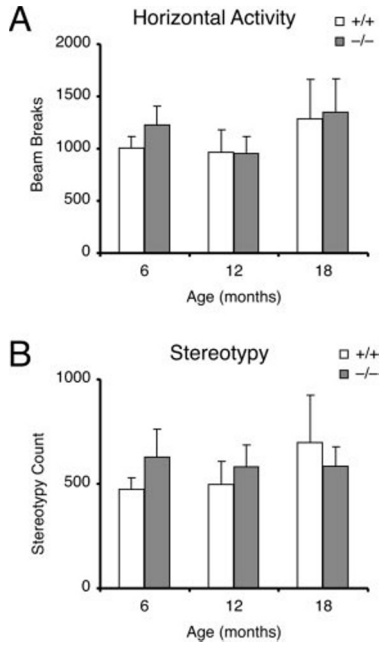

FIG. 2. **Open field test.** *parkin*−/− and wild-type mice exhibit similar levels of horizontal activity (*A*) and stereotypy (*B*) in 15-min trials.

tochemical analysis of *parkin*−/− brains using antibodies specific for synaptophysin, Munc-18 and calbindin showed grossly normal synaptic staining and striatum formation (data not shown). No inclusions were observed in any brain sub-regions, including the SN, using antibodies specific for α-synuclein and ubiquitin (data not shown).

Normal Neuroanatomy of DA Neurons in parkin−/− Mice—It has been proposed that the reduction in DA neurons in AR-JP could be due to impaired generation and maturation of these neurons, based on the observation that the remaining DA neurons in autopsies of AR-JP patients appear immature (18). Recently, *parkin*-null flies have also been shown to exhibit smaller dopaminergic neurons (36). Immunohistochemical analysis of *parkin*−/− mice using an antibody specific for TH, however, revealed normal morphology of DA neurons in the SN (Fig. 3, *C–F*) and noradrenaline neurons in the locus ceruleus (Fig. 3, *G* and *H*).

The most prominent neuropathological feature of AR-JP and PD is the selective loss of dopaminergic neurons in the SN (12–15). We therefore quantified the number of DA neurons in the SN of *parkin*−/− ($n = 4$) and control mice ($n = 4$) at 12, 18, and 24 months using unbiased stereological methods (27). Similar numbers of TH-positive neurons were found in the SN of *parkin*−/− and wild-type mice at 12 (+/+: 8520 ± 540; −/−: 8720 ± 710; $p > 0.05$), 18 (+/+: 8960 ± 450; −/−: 9360 ± 470; $p > 0.05$) and 24 months (+/+: 10500 ± 720; −/−: 10300 ± 1180; $p > 0.05$). We also measured the volume of DA neurons (+/+: $n = 47$; −/− $n = 50$) in the SN of 4 mice per genotype at age 24 months, and found similar neuron volumes between *parkin*−/− (2702 ± 150 μm^3) and wild-type (2674 ± 173 μm^3; $p > 0.05$) mice.

Increased Extracellular DA in the Striatum of parkin−/− Mice—We then looked for alterations in dopamine neurotransmission, which may occur prior to frank loss of dopaminergic neurons. Dopaminergic projections revealed by TH immunoreactivity appear normal in the striatum of *parkin*−/− mice (Fig. 3, *I* and *J*). Striatal levels of DA and its major metabolites, dihydroxyphenylacetic acid (DOPAC) and homovanillic acid (HVA) are similar between *parkin*−/− and control mice at 6, 12, 18, and 24 months ($p > 0.05$) (Fig. 4*A*). To determine whether there are alterations in dopamine release or reuptake,

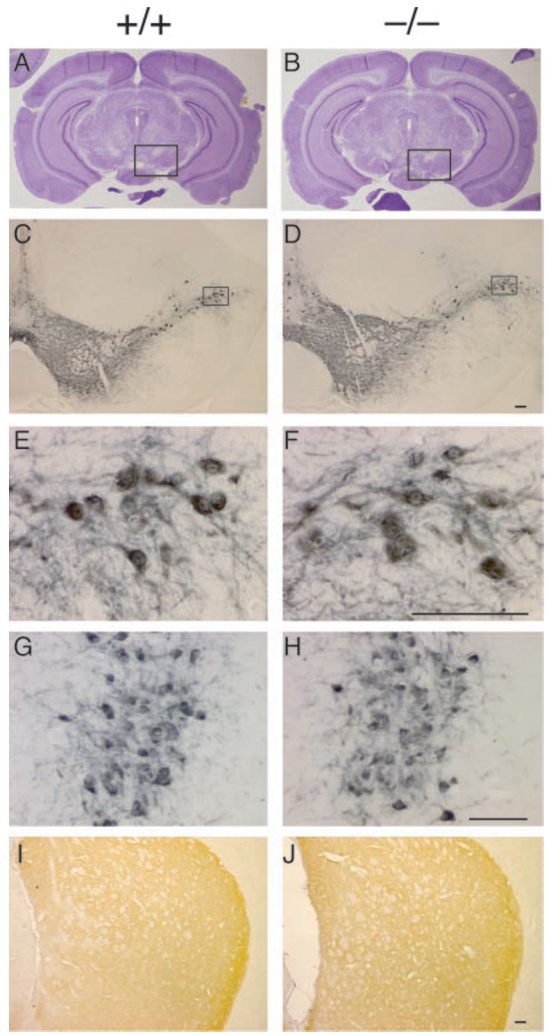

FIG. 3. **Normal neuroanatomy in *parkin*−/− brains.** *A* and *B*, Nissl-stained coronal brain sections at the level of the SN. *C* and *D*, higher power views of the boxed area in *A*, *B* showing normal TH immunoreactivity in the SN. *E* and *F*, higher power views of the *boxed area* in *C* and *D* showing normal morphology of dopaminergic neurons. *G* and *H*, similar TH immunoreactivity in the locus ceruleus. *I* and *J*, similar TH immunoreactivity in the striatum. Scale bar: 0.05 mm.

we performed no-net-flux microdialysis (37, 38) in the striatum of *parkin*−/− and wild-type mice at 8–9 months. When perfused with ACSF containing no DA, the dialysate DA concentration in *parkin*−/− mice ($n = 10$) (10.8 ± 1.2 nM) was significantly higher than that in wild-type mice ($n = 10$) (7.7 ± 0.4 nM; $p < 0.02$) (Fig. 4*B*).

The concentration of DA at the interpolated point of no-net-flux, a measure of extracellular DA concentration, was also significantly higher in *parkin*−/− mice ($n = 10$) (24.2 ± 1.2 nM) relative to wild-type controls ($n = 9$) (20.2 ± 0.9 nM; $p < 0.02$) (Fig. 4, *C* and *D*). The data from one wild-type mouse (indicated by an *arrow* in Fig. 4*C*), which met the statistical standard as an outlier (39), was excluded. The extraction fraction, a measure of DA reuptake, was not significantly different between wild-type (0.39 ± 0.04) and *parkin*−/− (0.46 ± 0.05; $p > 0.05$) mice (Fig. 4*E*). The elevated level of extracellular DA in *parkin*−/− mice, therefore, likely results from increased release of dopamine.

Unchanged Levels and Binding Affinities of D1 and D2 Receptors in the parkin−/− Striatum—We then examined whether the increase in extracellular DA results in an alteration of striatal DA receptors. Similar total receptor binding was found for both D1 and D2 receptors in the striatum of

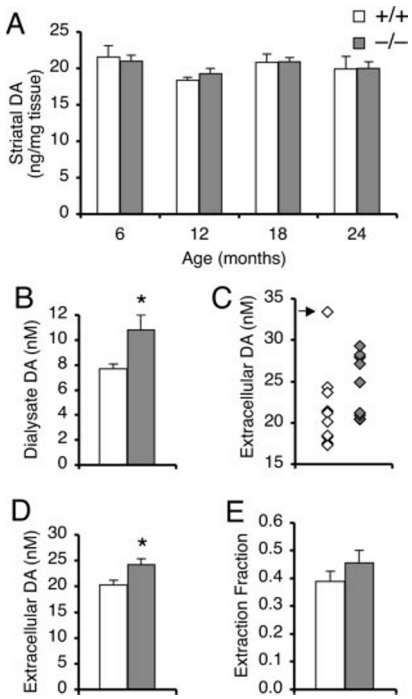

FIG. 4. Increased extracellular DA in the striatum of *parkin*−/− brains (*A*) HPLC quantification of striatal tissue content of DA. Values shown are means ± S.E. of *parkin*−/− and wild-type controls (4 per genotype for ages of 6 and 12 months, 7 per genotype for 18 months, 10 *parkin*−/− and 4 wild-type for 24 months). *B*, dialysate DA concentration following perfusion with DA-free ACSF. *Bars* show means ± S.E. for 10 *parkin*−/− and 10 wild-type mice (*asterisk*; $p < 0.02$, Student's *t* test). *C*, extracellular DA concentration determined by the point of no-net-flux for each mouse with a single statistical outlier in the wild-type group highlighted by the *arrow*. *D*, extracellular DA concentration (means ± S.E.) for 10 *parkin*−/− and 9 wild-type mice (*asterisk*; $p < 0.02$, Student's *t* test). *E*, extraction fractions determined by the slope of the linear regression line for each mouse. *Bars* show means ± S.E. for 10 *parkin*−/− and 9 wild-type mice ($p > 0.05$).

parkin−/− and control mice (B_{max} [fmol/mg], D1: 308 ± 65 *versus* 236 ± 34, D2: 347 ± 82 *versus* 328 ± 54 in +/+ and −/−, respectively; $n = 6$ for D1, $p = 0.35$; $n = 3$ for D2, $p = 0.85$). Examination of binding kinetics for D1 and D2 receptors similarly revealed no alterations in the affinity of either receptor (K_d [nM], D1: 1.60 ± 0.34 *versus* 1.06 ± 0.21, D2: 1.80 ± 0.46 *versus* 1.64 ± 0.32 in +/+ and −/−, respectively; $n = 6$ for D1, $p = 0.21$; $n = 3$ for D2, $p = 0.95$). These results suggest that there are no significant changes in DA receptor levels or binding affinities in *parkin*−/− mice, despite the increased extracellular concentration of DA.

Loss of parkin Decreases Synaptic Excitability of Striatal Neurons—The significant increase in extracellular DA in the striatum of *parkin*−/− mice prompted us to examine the electrophysiological responses of striatal neurons, as previous studies have demonstrated that the excitability of these neurons is strongly influenced by DA levels (40, 41). We focused our analysis on the medium-sized spiny neurons, which are the major neuronal subtype in the striatum. Major inputs received by these neurons include glutamatergic excitatory inputs from the cortex and dopaminergic inputs from the SN. Acute coronal corticostriatal slices were prepared from *parkin*−/− mice ($n = 7$) and wild-type controls ($n = 6$) at 6–9 months of age and striatal neurons (−/−: $n = 13$, +/+: $n = 10$) were examined by injecting current pulses intracellularly into each neuron (Fig. 5*A*). No significant differences in passive and active membrane properties were observed between the genotypes and all values were in the range of those reported in the literature for medium-sized spiny neurons (RMP: −78 ± 3 *versus* −80 ± 2 mV; input resistance: 29 ± 5 *versus* 37 ± 5 MOhms; AP amplitude: 66 ± 3 *versus* 68 ± 3 mV; AP width at 1/2 amplitude: 0.76 ± 0.03 *versus* 0.75 ± 0.07 ms; AHP amplitude: 11.7 ± 1.4 *versus* 12.1 ± 1.0 mV in +/+ *versus* −/− neurons, respectively) (Fig. 5*A*).

We then examined the synaptic response of the medium-sized spiny neuron by stimulation of corticostriatal afferents, the major glutamatergic excitatory pathway into the striatum. Although *parkin*−/− ($n = 13$) and wild-type ($n = 10$) neurons exhibited similar mean amplitudes and durations of evoked synaptic responses (peak amplitude: 9.9 ± 0.8 *versus* 10.5 ± 0.7 mV; peak duration at 1/2 amplitude: 9.05 ± 0.46 *versus* 9.22 ± 0.56 ms for +/+ *versus* −/− neurons, respectively) (Fig. 5*B*), higher currents were needed to evoke similar responses in *parkin*−/− neurons relative to the wild-type, as indicated by the significant rightward shift in the input-output relationships ($p < 0.02$) (Fig. 5*C*). The current required to evoke action potentials synaptically in *parkin*−/− neurons ($n = 10$; 720 ± 163 μA) was also significantly higher than in wild-type controls ($n = 12$; 202 ± 53 μA) ($p < 0.004$). These findings suggest that medium-sized striatal neurons are less excitable synaptically in *parkin*−/− mice. There were no differences in paired-pulse facilitation (50 ms interpulse interval) between wild-type (0.98 ± 0.06) and *parkin*−/− (1.02 ± 0.57) neurons, suggesting that the observed synaptic defect in *parkin*−/− mice may be caused by a postsynaptic alteration.

Behavioral Impairments in parkin−/− *Mice*—We further tested *parkin*−/− mice for possible alterations in motor activities using a beam traversal task, which is sensitive to impairment in the nigrostriatal pathway (42–45). Planned comparisons revealed that *parkin*−/− mice performed significantly worse than wild-type controls with higher numbers of slips and slips per step at all age groups ($p < 0.05$), while the number of steps was similar between the genotypic groups (Fig. 6, *A–C*). We further evaluated these mice in the rotarod task (46), which is commonly used to score severe motor impairments in rodents. *parkin*−/− and control mice exhibited similar latencies for remaining on the rotating rod (Fig. 6*D*).

Another test sensitive to nigrostriatal dysfunction in rodent models is the adhesive removal test, which assesses somatosensory abilities (47–49). *parkin*−/− mice at 2–4 and 7 months performed significantly worse compared with wild-type controls ($p < 0.05$), though the difference at 18 months was not as marked, likely due to the age-dependent decline of wild-type mice (Fig. 6*E*). Only 63% of wild-type mice at 18 months removed the middle size stimulus, compared with 100% at 4 months. This result is consistent with a previous report showing poorer performance by older animals (50).

Unchanged Levels of parkin Substrates—Recent *in vitro* studies have shown that parkin functions as an E3 ubiquitin ligase (21–23,26,51–54). Several proteins, such as CDCrel-1, synphilin-1, and glycosylated α-synuclein, have been shown to be ubiquitinylated by parkin *in vitro*. We therefore examined whether loss of parkin function results in accumulation of these proteins in *parkin*−/− mice. Western analysis showed similar levels of CDCrel-1, synphilin-1, and α-synuclein in *parkin*−/− and wild-type control brains (Fig. 7, *A–C*). Immunoprecipitation of α-synuclein followed by Western blotting using a second α-synuclein-specific antibody revealed the presence of an additional low abundance isoform at ~22 kDa, consistent with the apparent molecular weight of the glycosylated isoform of α-synuclein previously reported as a parkin substrate (26). No differences were observed in the steady state level of this higher molecular weight species between the genotypes (Fig. 7*D*). These results indicate that loss of parkin function does not affect the stead state level of any of these proteins in the mouse brain.

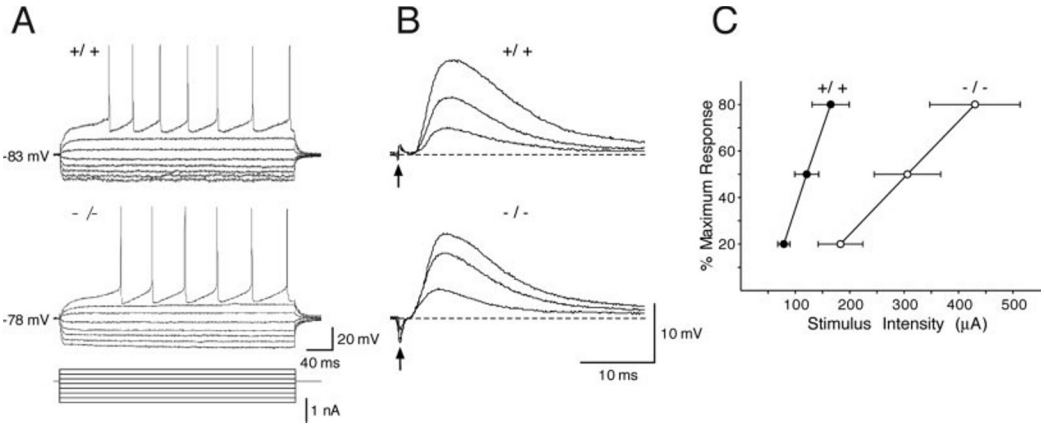

FIG. 5. **Electrophysiological deficits in *parkin*−/− mice.** *A*, current-voltage relationship of medium-sized striatal neurons recorded in acute slices, which was generated by injecting current pulses into each neuron and recording the change in induced voltages. No significant differences are found in current-voltage relationships or average passive and active membrane properties between *parkin*−/− and control neurons. Numbers to the *left* are RMPs for the two cells shown. *B*, depolarizing synaptic responses evoked by stimulation of corticostriatal afferents (*arrows* indicate the time of stimulation). *Traces* show no differences between the genotypes in superimposed representative response curves at ~20, 50, and 80% of the maximum amplitude (each curve is the average of at least 5 traces). *C*, normalized input-output relationship. *Filled circles* represent the intensity of the stimulation current (mean ± S.E.) needed to evoke responses at 20, 50, and 80% of the maximum postsynaptic potential in *parkin*−/− ($n = 13$) and wild-type ($n = 10$) neurons. Group differences at 50% ($p < 0.03$) and 80% ($p < 0.003$) were statistically significant (analysis of variance followed by post-hoc Student's t tests).

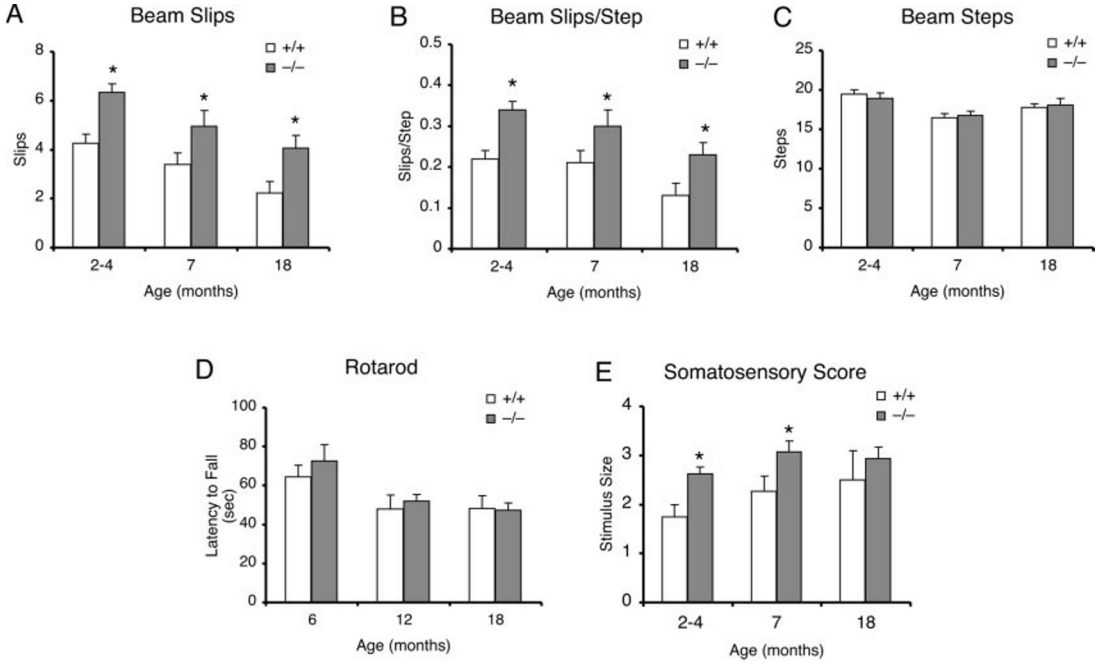

FIG. 6. **Behavioral deficits in *parkin*−/− mice.** *A*, slips; *B*, slips per step; and *C*, steps while traversing a narrowing mesh-covered beam. At ages 2–4 (+/+: $n = 9$, −/−: $n = 9$), 7 (+/+: $n = 10$, −/−: $n = 9$) and 18 months (+/+: $n = 7$, −/−: $n = 9$), *parkin*−/− mice had significantly more slips and slips per step compared with wild-type controls (*asterisks*; $p < 0.05$, Fisher's LSD). Values are means ± S.E. *D*, Rotarod performance is shown as the latency to fall off an accelerating rotating rod. The mean ± S.E. is shown for wild-type and *parkin*−/− mice at ages 6, 12, and 18 months ($n = 8$ per genotype at each age). *E*, somatosensory abilities scored according to the largest of five increasing sizes of adhesive that could not be detected and removed. Smaller numbers represent better performance. Mean scores are shown ± S.E. Pair-wise comparison of wild-type and *parkin*−/− mice within each age group shows significant impairment of *parkin*−/− mice at ages 2–4 (+/+: $n = 9$, −/−: $n = 9$) and 7 months (+/+: $n = 15$, −/−: $n = 14$) (*asterisks*; $p < 0.05$, Mann-Whitney U) but not at 18 months (+/+: $n = 8$, −/−: $n = 9$).

DISCUSSION

Despite a large body of evidence linking loss-of-function mutations of *parkin* to FPD, the normal physiological role of parkin and the mechanism by which parkin mutations cause nigral degeneration are unknown. Here we present three independent lines of evidence supporting a novel role of parkin in the nigrostriatal pathway. First, the extracellular DA concentration is significantly increased in the striatum of *parkin*−/− mice, which is likely due to an increase in dopamine release from nigral neurons. Second, the synaptic excitability of medium-sized spiny striatal neurons is reduced, as evidenced by increased currents required to evoke synaptic responses and action potentials. Lastly, *parkin*−/− mice exhibit deficits in behavioral tasks previously shown to be sensitive to nigrostriatal dysfunction (42–45, 47–49, 55, 56), although we cannot exclude the possibility that alterations in other neural circuits may also contribute to the observed behavioral deficits.

Together, these results indicate that parkin loss-of-function mutations cause defects in both DA release from nigral neurons and synaptic excitability of medium-sized spiny striatal neurons, which are the major target of nigral dopaminergic projections. Previous studies have shown that DA decreases gluta-

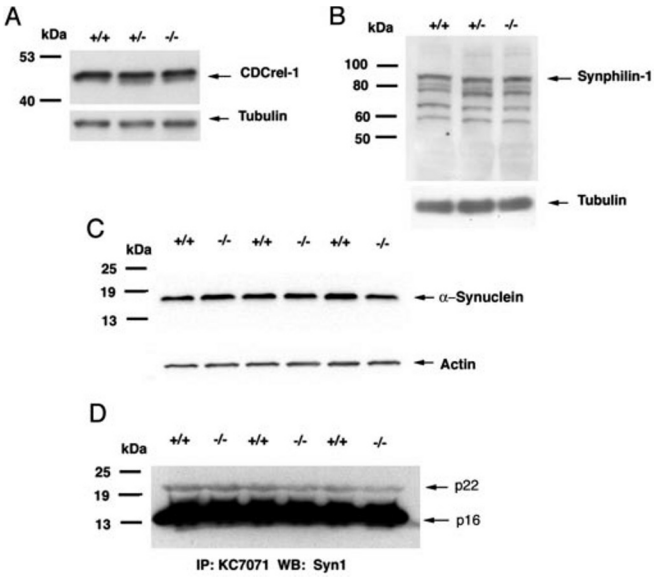

FIG. 7. **Similar levels of parkin substrates.** Western blot analysis of CDCrel-1 (*A*), synphilin-1 (*B*), and α-synuclein (*C*) shows similar steady-state levels of these proteins in brain homogenates from *parkin*−/− and wild-type mice. Immunoprecipitation of α-synuclein, followed by Western blotting reveals equivalent levels of a higher molecular size species at ~22 kDa that is immunoreactive for α-synuclein (*D*).

mate release and striatal excitability *via* activation of pre- and post-synaptic D2 family of dopamine receptors (41, 57), suggesting that the decreased excitability of striatal neurons in *parkin*−/− mice could be a consequence of the increased extracellular DA level in the striatum. The observation that parkin interacts with CASK *via* its PDZ-domain binding motif and associates with components of the glutamate receptor-signaling complex, such as PSD-95, NMDAR NR2B subunit, and CaMKII (58), also suggests a possible role for parkin in the regulation of synaptic transmission and plasticity. Several proteins that are enriched in presynaptic fractions, including CDCrel-1 (23), synphilin-1 (51), and α-synuclein (26), have been described *in vitro* as substrates for parkin-mediated ubiquitinylation. Although we did not observe an increase in the abundance of these substrates in *parkin*−/− brains (Fig. 7), parkin-mediated ubiquitinylation may regulate their activities in the synapse, possibly resulting in the observed synaptic phenotypes.

The cardinal neuropathological feature of PD, profound loss of dopaminergic neurons in the SN, is absent in *parkin*−/− mice. Thus, the mechanism underlying the mild motor deficits observed in *parkin*−/− mice may differ from the movement disorder characteristic of PD, which results primarily from substantial loss of DA neurons. Our results, however, are consistent with other mutant mice that exhibit decreased performance in beam traversal and increased concentrations of striatal DA (43). Mouse models of neurodegenerative diseases have previously been observed to recapitulate some aspects of the disease in the absence of substantial neuronal loss in the affected brain subregions. Transgenic mice overexpressing wild-type and FPD-linked mutant human α-synuclein exhibit motor deficits in the absence of loss of DA neurons (59–63). Similarly, genetically engineered mouse models of Alzheimer's (64) and Huntington's diseases (65) have successfully reproduced behavioral and neuropathological aspects of these diseases largely without recapitulating the cortical and striatal neuronal loss, respectively.

The fact that loss of parkin function alone in mice is insufficient to cause substantial loss of dopamine neurons suggests that other factors also contribute to nigral degeneration. One possibility is that parkin protects neurons from various insults, which has been observed by overexpressing parkin in transfected cells (66, 67) and transgenic flies (68). However, no decrease in DA neuron survival has been observed in *Drosophila* in which endogenous *parkin* has been inactivated (36) or partially inactivated by RNAi (68), consistent with our findings in *parkin*−/− mice. Together, these findings suggest that additional events may be required for neuronal degeneration. This notion is also consistent with the fact that the age of onset for FPD patients carrying *parkin* mutations ranges from juvenile to elderly and varies by as much as 20 years even within single families (9). Other possibilities, including higher tolerance to neuronal degeneration in the mouse DA neuron, shorter life span of mice, and the well-controlled environment in which these mice are housed, may also contribute to the absence of the profound nigral degeneration characteristic of PD brains.

In summary, our findings provide important insights into the normal physiological role of parkin in dopamine regulation and nigrostriatal function, which will facilitate the exploration of the mechanisms of PD pathogenesis and may assist the identification of novel preventative and therapeutic strategies.

Acknowledgments—We thank A. Martins and L. Cai for technical assistance and M. Irizarry and B. Hyman for advice and use of stereological neuron counting system.

REFERENCES

1. Fahn, S., and Cohen, G. (1992) *Ann. Neurol.* **32,** 804–812
2. Kosel, S., Hofhaus, G., Maassen, A., Vieregge, P., and Graeber, M. B. (1999) *Biol. Chem.* **380,** 865–870
3. Tanner, C. M., and Langston, J. W. (1990) *Neurology* **40,** 17–30
4. Polymeropoulos, M. H., Lavedan, C., Leroy, E., Ide, S. E., Dehejia, A., Dutra, A., Pike, B., Root, H., Rubenstein, J., Boyer, R., Stenroos, E. S., Chandrasekharappa, S., Athanassiadou, A., Papapetropoulos, T., Johnson, W. G., Lazzarini, A. M., Duvoisin, R. C., Diiorio, G., Golbe, L. I., and Nussbaum, R. L. (1997) *Science* **276,** 2045–2047
5. Kitada, T., Asakawa, S., Hattori, N., Matsumine, H., Yamamura, Y., Minoshima, S., Yokochi, M., Mizuno, Y., and Shimizu, N. (1998) *Nature* **392,** 605–608
6. Bonifati, V., Rizzu, P., van Baren, M. J., Schaap, O., Breedveld, G. J., Krieger, E., Dekker, M. C., Squitieri, F., Ibanez, P., Joosse, M., van Dongen, J. W., Vanacore, N., van Swieten, J. C., Brice, A., Meco, G., van Duijn, C. M., Oostra, B. A., and Heutink, P. (2003) *Science* **299,** 256–259
7. Abbas, N., Lucking, C. B., Ricard, S., Durr, A., Bonifati, V., De Michele, G., Bouley, S., Vaughan, J. R., Gasser, T., Marconi, R., Broussolle, E., Brefel-Courbon, C., Harhangi, B. S., Oostra, B. A., Fabrizio, E., Bohme, G. A., Pradier, L., Wood, N. W., Filla, A., Meco, G., Denefle, P., Agid, Y., Brice, A. (1999) *Hum. Mol. Genet.* **8,** 567–574
8. Hattori, N., Kitada, T., Matsumine, H., Asakawa, S., Yamamura, Y., Yoshino, H., Kobayashi, T., Yokochi, M., Wang, M., Yoritaka, A., Kondo, T., Kuzuhara, S., Nakamura, S., Shimizu, N., and Mizuno, Y. (1998) *Ann. Neurol.* **44,** 935–941
9. Lucking, C. B., Durr, A., Bonifati, V., Vaughan, J., De Michele, G., Gasser, T., Harhangi, B. S., Meco, G., Denefle, P., Wood, N. W., Agid, Y., and Brice, A. (2000) *N. Engl. J. Med.* **342,** 1560–1567
10. West, A., Periquet, M., Lincoln, S., Lucking, C. B., Nicholl, D., Bonifati, V., Rawal, N., Gasser, T., Lohmann, E., Deleuze, J. F., Maraganore, D., Levey, A., Wood, N., Durr, A., Hardy, J., Brice, A., and Farrer, M. (2002) *Am. J. Med. Genet.* **114,** 584–591
11. Klein, C., Pramstaller, P. P., Kis, B., Page, C. C., Kann, M., Leung, J., Woodward, H., Castellan, C. C., Scherer, M., Vieregge, P., Breakefield, X. O., Kramer, P. L., and Ozelius, L. J. (2000) *Ann. Neurol.* **48,** 65–71
12. Hayashi, S., Wakabayashi, K., Ishikawa, A., Nagai, H., Saito, M., Maruyama, M., Takahashi, T., Ozawa, T., Tsuji, S., and Takahashi, H. (2000) *Mov. Disord.* **15,** 884–888
13. Mori, H., Kondo, T., Yokochi, M., Matsumine, H., Nakagawa-Hattori, Y., Miyake, T., Suda, K., and Mizuno, Y. (1998) *Neurology* **51,** 890–892
14. Takahashi, H., Ohama, E., Suzuki, S., Horikawa, Y., Ishikawa, A., Morita, T., Tsuji, S., and Ikuta, F. (1994) *Neurology* **44,** 437–441
15. van de Warrenburg, B. P., Lammens, M., Lucking, C. B., Denefle, P., Wesseling, P., Booij, J., Praamstra, P., Quinn, N., Brice, A., and Horstink, M. W. (2001) *Neurology* **56,** 555–557
16. Farrer, M., Chan, P., Chen, R., Tan, L., Lincoln, S., Hernandez, D., Forno, L., Gwinn-Hardy, K., Petrucelli, L., Hussey, J., Singleton, A., Tanner, C., Hardy, J., and Langston, J. W. (2001) *Ann. Neurol.* **50,** 293–300
17. Kitada, T., Asakawa, S., Minoshima, S., Mizuno, Y., and Shimizu, N. (2000) *Mamm. Genome* **11,** 417–421
18. Kitada, T., Asakawa, S., Matsumine, H., Hattori, N., Shimura, H., Minoshima, S., Shimizu, N., and Mizuno, Y. (2000) *Neurogenetics* **2,** 207–218
19. Solano, S. M., Miller, D. W., Augood, S. J., Young, A. B., and Penney, J. B., Jr. (2000) *Ann. Neurol.* **47,** 201–210
20. Shimura, H., Hattori, N., Kubo, S., Yoshikawa, M., Kitada, T., Matsumine, H., Asakawa, S., Minoshima, S., Yamamura, Y., Shimizu, N., and Mizuno, Y.

(1999) *Ann. Neurol.* **45,** 668–672
21. Imai, Y., Soda, M., and Takahashi, R. (2000) *J. Biol. Chem.* **275,** 35661–35664
22. Shimura, H., Hattori, N., Kubo, S., Mizuno, Y., Asakawa, S., Minoshima, S., Shimizu, N., Iwai, K., Chiba, T., Tanaka, K., and Suzuki, T. (2000) *Nat. Genet.* **25,** 302–305
23. Zhang, Y., Gao, J., Chung, K. K., Huang, H., Dawson, V. L., and Dawson, T. M. (2000) *Proc. Natl. Acad. Sci. U. S. A.* **97,** 13354–13359
24. Yu, H., Kessler, J., and Shen, J. (2000) *Genesis* **26,** 5–8
25. Yu, H., Saura, C. A., Choi, S.-Y., Sun, L. D., Yang, X., Handler, M., Kawarabayashi, T., Younkin, L., Fedeles, B., Wilson, M. A., Younkin, S., Kandel, E. R., Kirkwood, A., and Shen, J. (2001) *Neuron* **31,** 713–726
26. Shimura, H., Schlossmacher, M. G., Hattori, N., Frosch, M. P., Trockenbacher, A., Schneider, R., Mizuno, Y., Kosik, K. S., and Selkoe, D. J. (2001) *Science* **293,** 263–269
27. Sterio, D. (1983) *J. Microsc.* **134,** 127–136
28. Murphy, N. P., Lam, H. A., and Maidment, N. T. (2001) *J. Neurochem.* **79,** 626–635
29. Shapiro, D. A., Renock, S., Arrington, E., Chiodo, L. A., Liu, L. X., Sibley, D. R., Roth, B. L., and Mailman, R. (2003) *Neuropsychopharmacology* **28,** 1400–1411
30. Roth, B. L., McLean, S., Zhu, X. Z., and Chuang, D. M. (1987) *J. Neurochem.* **49,** 1833–1838
31. Roth, B. L., Baner, K., Westkaemper, R., Siebert, D., Rice, K. C., Steinberg, S., Ernsberger, P., and Rothman, R. B. (2002) *Proc. Natl. Acad. Sci. U. S. A.* **99,** 11934–11939
32. Klapstein, G. J., Fisher, R. S., Zanjani, H., Cepeda, C., Jokel, E. S., Chesselet, M. F., and Levine, M. S. (2001) *J. Neurophysiol.* **86,** 2667–2677
33. Asakawa, S., Tsunematsu, K., Takayanagi, A., Sasaki, T., Shimizu, A., Shintani, A., Kawasaki, K., Mungall, A. J., Beck, S., Minoshima, S., and Shimizu, N. (2001) *Biochem. Biophys. Res. Commun.* **286,** 863–868
34. Kozak, M. (2001) *Nucleic Acids Res.* **29,** 5226–5232
35. Finney, N., Walther, F., Mantel, P. Y., Stauffer, D., Rovelli, G., and Dev, K. K. (2003) *J. Biol. Chem.* **278,** 16054–16058
36. Greene, J. C., Whitworth, A. J., Kuo, I., Andrews, L. A., Feany, M. B., and Pallanck, L. J. (2003) *Proc. Natl. Acad. Sci. U. S. A.* **100,** 4078–4083
37. Cosford, R. J., Vinson, A. P., Kukoyi, S., and Justice, J. B., Jr. (1996) *J. Neurosci. Methods* **68,** 39–47
38. Parsons, L. H., and Justice, J. B., Jr. (1994) *Crit. Rev. Neurobiol.* **8,** 189–220
39. Hadi, A. S. (1992) *J. Royal Statistical Society, Series B* **3,** 761–771
40. Calabresi, P., Mercuri, N., Stanzione, P., Stefani, A., and Bernardi, G. (1987) *Neuroscience* **20,** 757–771
41. Levine, M. S., Li, Z., Cepeda, C., Cromwell, H. C., and Altemus, K. L. (1996) *Synapse* **24,** 65–78
42. Garcia-Hernandez, F., Pacheco-Cano, M. T., and Drucker-Colin, R. (1993) *Physiol. Behav.* **54,** 589–598
43. Dluzen, D. E., Gao, X., Story, G. M., Anderson, L. I., Kucera, J., and Walro, J. M. (2001) *Exp. Neurol.* **170,** 121–128
44. Drucker-Colin, R., and Garcia-Hernandez, F. (1991) *J. Neurosci. Methods* **39,** 153–161
45. Walsh, S. L., and Wagner, G. C. (1992) *J. Pharmacol. Exp. Ther.* **263,** 617–626
46. Dunham, N. W., and Miya, T. S. (1957) *J. Am. Pharmacol. Assoc.* **46,** 208–209
47. Schallert, T., Upchurch, M., Lobaugh, N., Farrar, S. B., Spirduso, W. W., Gilliam, P., Vaughn, D., and Wilcox, R. E. (1982) *Pharmacol. Biochem. Behav.* **16,** 455–462
48. Schallert, T., Upchurch, M., Wilcox, R. E., and Vaughn, D. M. (1983) *Pharmacol. Biochem. Behav.* **18,** 753–759
49. Schallert, T., Fleming, S. M., Leasure, J. L., Tillerson, J. L., and Bland, S. T. (2000) *Neuropharmacology* **39,** 777–787
50. Schallert, T. (1988) in *Annals of the New York Academy of Science: Central Determinants of Age-Related Decline in Motor Function* (Joseph, J. A., ed) Vol. 515, pp. 108–120, New York Academy of Sciences, New York
51. Chung, K. K., Zhang, Y., Lim, K. L., Tanaka, Y., Huang, H., Gao, J., Ross, C. A., Dawson, V. L., and Dawson, T. M. (2001) *Nat. Med.* **7,** 1144–1150
52. Imai, Y., Soda, M., Inoue, H., Hattori, N., Mizuno, Y., and Takahashi, R. (2001) *Cell* **105,** 891–902
53. Ren, Y., Zhao, J., and Feng, J. (2003) *J. Neurosci.* **23,** 3316–3324
54. Corti, O., Hampe, C., Koutnikova, H., Darios, F., Jacquier, S., Prigent, A., Robinson, J. C., Pradier, L., Ruberg, M., Mirande, M., Hirsch, E., Rooney, T., Fournier, A., and Brice, A. (2003) *Hum. Mol. Genet.* **12,** 1427–1437
55. Ljungberg, T., and Ungerstedt, U. (1976) *Exp. Neurol.* **53,** 585–600
56. Schallert, T., and Tillerson, J. L. (1999) in *Central Nervous System Diseases* (Emerich, D. F., Dean, R. L., and Sandberg, P. R., eds) pp. 131–151, Humana Press, Inc., Totowa
57. Cepeda, C., Hurst, R. S., Altemus, K. L., Flores-Hernandez, J., Calvert, C. R., Jokel, E. S., Grandy, D. K., Low, M. J., Rubinstein, M., Ariano, M. A., and Levine, M. S. (2001) *J. Neurophysiol.* **85,** 659–670
58. Fallon, L., Moreau, F., Croft, B. G., Labib, N., Gu, W. J., and Fon, E. A. (2002) *J. Biol. Chem.* **277,** 486–491
59. Masliah, E., Rockenstein, E., Veinbergs, I., Mallory, M., Hashimoto, M., Takeda, A., Sagara, Y., Sisk, A., and Mucke, L. (2000) *Science* **287,** 1265–1269
60. van Der Putten, H., Wiederhold, K. H., Probst, A., Barbieri, S., Mistl, C., Danner, S., Kauffmann, S., Hofele, K., Spooren, W. P., Ruegg, M. A., Lin, S., Caroni, P., Sommer, B., Tolnay, M., and Bilbe, G. (2000) *J. Neurosci.* **20,** 6021–6029
61. Richfield, E. K., Thiruchelvam, M. J., Cory-Slechta, D. A., Wuertzer, C., Gainetdinov, R. R., Caron, M. G., Di Monte, D. A., and Federoff, H. J. (2002) *Exp. Neurol.* **175,** 35–48
62. Giasson, B. I., Duda, J. E., Quinn, S. M., Zhang, B., Trojanowski, J. Q., and Lee, V. M. (2002) *Neuron* **34,** 521–533
63. Lee, M. K., Stirling, W., Xu, Y., Xu, X., Qui, D., Mandir, A. S., Dawson, T. M., Copeland, N. G., Jenkins, N. A., and Price, D. L. (2002) *Proc. Natl. Acad. Sci. U. S. A.* **99,** 8968–8973
64. Hock, B. J., Jr., and Lamb, B. T. (2001) *Trends Genet.* **17,** S7–12
65. Menalled, L. B., and Chesselet, M. F. (2002) *Trends Pharmacol. Sci.* **23,** 32–39
66. Staropoli, J. F., McDermott, C., Martinat, C., Schulman, B., Demireva, E., and Abeliovich, A. (2003) *Neuron* **37,** 735–749
67. Petrucelli, L., O'Farrell, C., Lockhart, P. J., Baptista, M., Kehoe, K., Vink, L., Choi, P., Wolozin, B., Farrer, M., Hardy, J., and Cookson, M. R. (2002) *Neuron* **36,** 1007–1019
68. Yang, Y., Nishimura, I., Imai, Y., Takahashi, R., and Lu, B. (2003) *Neuron* **37,** 911–924